Photoemission studies of layered transition-metal dichalcogenides: MoS_2†

J. C. McMenamin* and W. E. Spicer
Stanford Electronic Laboratories, Stanford University, Stanford, California 94305
(Received 20 June 1977)

Ultraviolet photoemission spectroscopy (UPS) has been used to study the valence-band electronic structure of $2H$-MoS_2. The samples were cleaved or heated in ultrahigh vacuum of $\sim 1 \times 10^{-10}$ Torr to achieve atomically clean surfaces. A spherical retarding-field analyzer was used to measure the angle-integrated photoelectron energy-distribution curves (EDC) and Fermi levels were located by the use of a copper reference sample. In $2H$-MoS_2, EDC structure is observed primarily at constant initial-state energies but with relative strengths being a strong function of photon energy. Arguments are presented that these data are indicative of bulk MoS_2 electronic structure. The data can thus provide a sensitive test for a detailed calculation of MoS_2 bulk electronic structure and transition probabilities. The UPS data are combined with other reported data, and a rather complete band model for MoS_2 is developed. Two key points of this model are a semiconducting band gap in excess of 1 eV and an overlap of the two valence bands. This model is compared with earlier models (such as Wilson and Yoffe's) as well as more recent "first-principles" band-structure calculations.

I. INTRODUCTION

The layered transition-metal dichalcogenides form a family of compounds having the chemical formula TX_2, where T represents a transition metal from group IV, V, or VI, and X represents a chalcogen—S, Se, or Te. The most striking feature of this family of compounds is their highly anisotropic layer structure, which consists of chalcogen-metal-chalcogen "sandwiches" bonded to each other by weak Van der Waals–type forces. Since the bonding within the "sandwiches" is strongly covalent the crystals readily cleave along a Van der Waals gap.[1] Because none of the covalent bonds are broken by such a cleave the exposed surfaces are relatively inert with no "dangling bonds." The properties of these materials have been extensively reviewed by Wilson and Yoffe[1] and more recently by Yoffe.[2]

Several simple models have been proposed for the TX_2 compounds. Goodenough[3] first proposed a model based on crystal-field theory, and semiempirical models based on molecular orbitals were proposed by Huisman *et al.*[4] and Connell *et al.*[5] but the model which received the strongest early acceptance was the rigid-band model proposed by Wilson and Yoffe[1] (WY). In their study, Wilson and Yoffe[1] correlated the visible transmission spectra and the electrical and structural properties of the TX_2 compounds to develop a useful band model consistent with a molecular-orbital approach. This model gained added importance since it was used as the basis for several "semiempirical" band-structure calculations using the tight-binding approximation.[6-8]

In a previous paper[9] the present authors reported preliminary ultraviolet-photoemission-spectroscopy (UPS) data which were not consistent with several aspects of the WY model for MoS_2.[1] In particular, the band gaps and bandwidths deduced by WY were not in agreement with our UPS data. Because semiempirical band calculations are often fit to the band gaps and widths of a simple model, it is important that these parameters be known accurately, or the entire calculation can be affected. For this reason, we proposed modifications to the WY model[1] which have since met with some opposition based on suggestions that our UPS data[9] were not indicative of bulk MoS_2 electronic structure and might be misleading.[2,10] In this work we report addional UPS data for MoS_2 to support our previous position,[9] and we compare our results with photoemission data from other groups[11-13] and with more recent "first-principles" band calculations.[10,14-16]

Figure 1 shows schematically the band model originally proposed by WY for TX_2 compounds with trigonal-prism structure. In this model, the electrical properties are determined by the degree of filling of narrow "nonbonding" d bands lying in the basic bonding-antibonding band gap. The dashed lines in Fig. 1 indicate the Fermi level for the metal group-V compounds and for the semiconducting group-VI compounds. Since the atomic character of the bands appears to be much more complex than the WY notation implies, we have chosen to label the so-called d_z^2 band as V_1 and the lower valence band V_2. Likewise, we label the mainly metal p-d band as C_1 and the higher conduction bands C_2. For MoS_2, WY deduce a 0.27-eV semiconducting gap with an upper filled band V_1 about 0.8 eV wide and separated by about 0.9 eV from the lower valence band V_2.[1] They also suggest that the sharp excitonic structure just below the visible absorption edge is due to transitions from the top of V_2 to the bottom of C_1.

Although WY have fit this model to their inter-

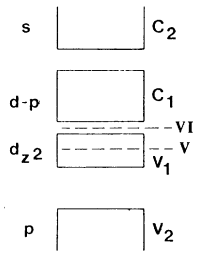

FIG. 1. Band model for trigonal-prismatic TX_2. Compounds originally proposed by Wilson and Yoffe (Ref. 1). The dashed lines labeled V and VI locate the position of the Fermi level in group-V and group-VI transition-metal compounds, respectively.

pretation of their optical data, the optical data have a basic ambiguity in that they measure only energy *differences* between valence- and conduction-band features and not the energies of the individual features, as is the case with photoemission. Because of this ambiguity, it was possible for WY to fit their optical data to a model which is inconsistent with photoemission data such as those reported here. (We should also point out that some discrepancies with the WY optical data have been reported. For example, Huisman *et al.* have failed to observe the 0.27-eV absorption edge but instead find an absorption edge at 1.35 eV.[4])

After discussing our experimental methods in Sec. II, we present our photoemission data in Sec. III. The inconsistencies between our data and the WY model, and the objections made to our previously reported[9] data will be discussed as the data are presented. In Sec. IV we compare our results with data from complementary experiments and then, in Sec. V, we develop our model for the electronic structure of MoS_2. An appendix to this paper considers the effects of surface contamination on the photoemission results for MoS_2.

II. EXPERIMENTAL METHODS

The ultrahigh-vacuum photoemission chamber used for this work was a modification of the chamber developed by Powell[17] and Derbenwick.[18] The chamber utilizes a spherical analyzer to measure the photoelectron energy-distribution curves (EDC) with an ac-modulated retarding-field technique similar to that of Eden.[19] It should be noted here that the spherical energy analyzer has the advantage of collecting photoelectrons emitted from all angles rather than only a small sample of angles, as many other analyzers do. Thus angular effects,[20,21] which are very strong in layer compounds,[12,22,23] are integrated out, and no photoelectrons are lost from the distributions. This is an important consideration in the present work since Yoffe[2] has specifically suggested that angular effects in UPS experiments may be the source of disagreement between some aspects of his electronic-structure model for MoS_2 (Refs. 1 and 2) and our UPS results.[9] The only directional effect in our experiments was that the incident light beam was constrained to be approximately normal to the cleavage plane of the layer crystal so that the electric field vector $\vec{E}$ lies approximately in the cleavage plane; but it has been argued theoretically[21] that this should affect only the intensity and not the position of structure in the EDC's. In addition, the light divergence and sample alignment are such that the light is in the range of 0°–6° to the normal so that transitions which are "forbidden" for $\vec{E} \perp \vec{c}$ should still be weakly excited (reduced about one order of magnitude from maximum).

An important feature of the chamber is a clean copper back shutter (prepared by *in situ* evaporation). Photoelectron EDC's from this back shutter can be used to locate accurately the energy of the Fermi level (E_F).[24] The modifications to the chamber include an aperture to restrict the size of the incident light beam to the relatively small (~5-mm-diam.) samples and provisions for cleaving layer crystals in ultrahigh vacuum (~10^{-10} Torr) by means of a flexible copper strap attached to the front surface of the crystal with indium-alloy solder.[25] It was found that solders with high (>50%) indium content adhere well to most TX_2 compounds if an ultrasonic soldering iron is used.[26] The full-width-at-half-maximum (FWHM) resolution of the analyzer is about 0.15 eV for electrons with kinetic energy near zero. At higher electron energies the resolution is degraded to about 0.3 eV for 15-eV electrons and 0.5 eV for 35-eV electrons. The energies of peaks in most of the EDC's can be determined to within ±0.1 eV relative to each other; however, absolute energies relative to E_F (as determined by the copper back shutter[24]) have an uncertainty of about ±0.2 eV because the measured energy of an electron photoemitted from the sample is somewhat sensitive to the position of the sample within the spherical collector can.

For photon energies above 11.8 eV (high-energy transmission cutoff of LiF), a two-stage differentially pumped resonance lamp was used as a photon source.[27] Intense spectral lines are obtained with He at 21.2 and 40.8 eV and with Ne at 16.8 eV. With the gas supply to the lamp turned off, the chamber could be evacuated to a pressure of 2×10^{-10} Torr. During lamp operation the chamber pressure increases to ~4×10^{-9} Torr; however, mass-spectrometer analysis shows most of the pressure rise is due to the inert discharge gas (He or Ne). Further evidence for the cleanliness of this lamp is that no contamination has been obser-

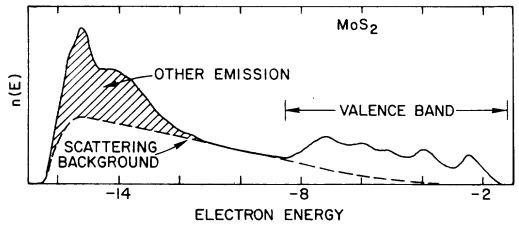

FIG. 2. Full EDC from MoS_2 at 21.2-eV photon energy. The shaded portion shows the electron emission from low-energy photons emitted by impurities in the gas discharge.

ved after 8 h of lamp operation, even with relatively active samples such as Cu or Pt.[28] This rate of contamination is comparable to the rate of contamination without the lamp. (The presence of surface contamination of ~0.1 monolayer can be readily detected with UPS at these photon energies.)

A major limitation of the lamp was considerable output of lower-energy spectral lines due to H_2 impurity in the lamp discharge. These lines at 12.6, 10.2, and 7.7 eV cause extra photoelectrons to be emitted near threshold, making it difficult to obtain useful data in that region. Figure 2 shows the entire distribution of photoemitted electrons from MoS_2 using He in the resonance lamp. The shaded area is the approximate emission from the lower-energy photons. The emission from low-energy photons was determined by measuring an EDC with a LiF filter in front of the He lamp.[28] This EDC was scaled up to account for the absorption of the LiF filter, and then subtracted from an EDC measured without a filter. This left a nearly smooth scattering background with several small peaks which corresponded to peak locations expected from ~12 to 14-eV photons. Under these small peaks a smooth curve approximating the scattering from 21.2-eV emission could be extrapolated. The dashed curve in Fig. 2 indicates this estimation of the contribution from scattered electrons.

For $h\nu \leq 11.8$ eV, a low-vacuum McPhearson 225 monochromator was used with a hot-filament H_2 discharge light source similar to the one described by Eastman and Donelon.[29] A LiF window[30] was used to isolate the ultrahigh-vacuum chamber from the monochromator vacuum, thus allowing the cleaned sample to be kept at a pressure below 1×10^{-10} Torr at all times.

The quantum yield per incident photon below 11.8 eV was measured with a calibrated Cs_3Sb photodiode.[31] Since an aperture was used on the chamber, not all of the light incident on the photodiode reached the sample. We corrected for this effect by measuring the yield of the collector back shutter with the aperture in place and comparing it at each photon energy to the yield of an identically prepared sample without an aperture. This procedure leads to corrections of about ±20% in the absolute quantum yield; however, the corrections are slowly varying with photon energy, and no structure in the yield is significantly affected. When measuring the yield below 7-eV photon energy, it was essential to use a quartz filter on the output of the monochromator to eliminate scattered high-energy photons and higher-order diffraction. Without the use of the quartz filter, spurious photocurrent could be detected several eV below the actual photothreshold.

In the ac-modulated retarding-field technique for photoemission,[19] the first derivative of the EDC can be obtained directly by tuning the phase-sensitive detector to the second harmonic of the modulation frequency.[32] The first derivative EDC (dEDC) has the advantage that it accentuates weak features not easily visible in the EDC itself. (Of course, one must take care to use the dEDC's only in conjunction with the EDC's to avoid being misled into thinking that a feature in the dEDC is a major one when, in fact, it is a very small feature of the electronic structure.) The derivative technique is most useful in following the energy of a piece of structure in the EDC's over changing photon energy because it allows a feature to be consistently located in energy even though, for some photon energies, the feature becomes nearly obscured or overlapped by other stronger structure.

Figure 3 shows an EDC for MoS_2 at photon energy $h\nu = 10.2$ eV. The weak structures labeled A' and S are not apparent in the EDC (dashed) but are clear in the first derivative (solid). At first one might think that structures A' and S are too small to be important, but at other photon energies the relative transition probabilities are such that A'

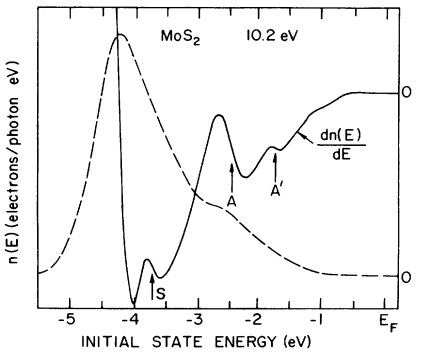

FIG. 3. EDC (dashed) and its derivative (dEDC) measured at 10.2-eV. Features A' and S in the dEDC are too weak to be obvious in the EDC at this energy; however, features at the same initial-state energies as A' and S are easily observed in EDC's at other photon energies.

and S are clearly visible even in the EDC. Since the derivative allows us to locate A' and S even when they are obscured in the EDC, we can observe the movement of the kinetic energy of A' and S with $h\nu$ over a wide range and can, therefore, associate these features with the initial density of states.[33] To be consistent, the energy of a feature in the derivative is taken as the energy of the midpoint of the downward sloping portion of the "wiggle" (MDSW) associated with the feature. The main justification for defining the energy of a feature in the derivative EDC as the MDSW is that it is unambiguous and can be located precisely. In addition, whenever a peak is clearly resolved in the EDC, the energy of that peak is the same as the corresponding MDSW in the dEDC. The use of the MDSW is especially helpful in deconvolving a curve into several symmetric functions since, in that case, a MDSW corresponds to a peak in one of the functions. Although the MDSW is useful in analyzing the dEDC features, it must be related to the actual electronic density of states (DOS) cautiously since, in general, one cannot assume that the DOS is a sum of individual symmetric peaks.

III. PHOTOEMISSION RESULTS FOR MoS_2

Natural molybdenite was used for all our MoS_2 experiments since it is readily available in large single crystals with $2H$ stacking arrangement. The samples were generously supplied by Acrivos of San Jose State University, who found them to have unusually small amounts of impurities.[34] The low-energy ($h\nu < 11.8$-eV) data were all obtained on samples which were cleaved in ultrahigh-vacuum (UHV) of 4×10^{-10} Torr. It was found, however, that samples cleaved in air and subsequently heat cleaned in a vacuum of $\sim 10^{-10}$ Torr for 6 h at 400 °C gave identical results. Since this heat-cleaning technique is simpler and more reliable, it was used to prepare all of the samples for the high-energy ($h\nu > 11.8$-eV) data. (The effects of surface contamination are discussed in the Appendix of this paper.)

Since photon energies less than 11.8 eV are insufficient to probe the entire valence band of MoS_2, we will first present the "high-energy" ($h\nu > 11.8$-eV) photoemission EDC's taken with the windowless lamp as described in Sec. II. Besides being able to probe the entire valence band, these "high-energy" EDC's have the added advantages that (i) the background secondary electrons can be readily separated from the primary emission, (ii) EDC structure caused by final-state density is minimized, and (iii) "direct-transition" effects[33] tend to be averaged out so that the EDC's more closely resemble the valence-band density of states (DOS). The "low-energy" EDC's will be presented subsequently to show the changes in EDC's which occur for small changes in photon energy. The shift in an EDC structure with photon energy can then be used to deduce the origin of that structure.[33] Since the EDC structure depends on initial-state density, final-state density, and optical-transition probability, the shift in EDC structure with photon energy can be used to gain information on the final-state density and transition probability in addition to deducing valence band DOS.[33] Additionally, the "low-energy" UPS data can often be combined with uv optical data to gain further information on both the filled and empty electronic states.

Figure 4 shows the valence-band emission for photon energies ($h\nu$) of 16.8, 21.2, and 40.8 eV. The horizontal scale gives the initial-state energy of the electron relative to the Fermi level (E_F) as determined from the back shutter of the electron energy analyzer.[24] The dashed line indicates the estimated contribution of scattered electrons to the EDC at 16.8 eV. Since we were not equipped to measure the incident light intensity at these photon energies, the EDC's have been arbitrarily normalized to have the same area (after subtraction of the scattering contribution). The data at 16.8 and 21.2 eV were virtually noise free (signal-to-noise ratio of ~200) with an energy uncertainty of ±0.1 eV. The data at 40.8 eV, however, were quite noisy, so a smoothed average of several runs was used to prepare the 40.8-eV curve in Fig. 4. This curve has an estimated energy uncertainty of ±0.3 eV.

To aid analysis, the UPS EDC's of Fig. 4 with the scattering background subtracted have been presented in Fig. 5 along with the $h\nu = 1486.6$-eV x-ray-photoemission-spectroscopy (XPS) data of

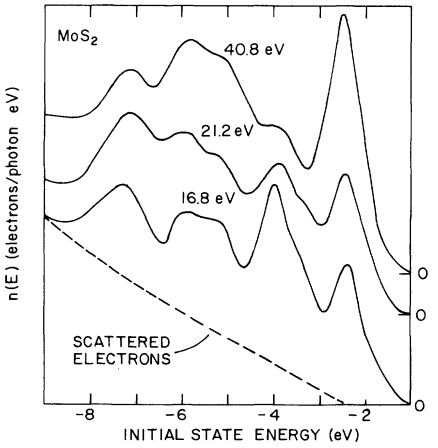

FIG. 4. MoS_2 valence-band EDC's taken with the resonance lamp. The dashed line shows the approximate contribution of scattered electrons to the 16.8-eV curve.

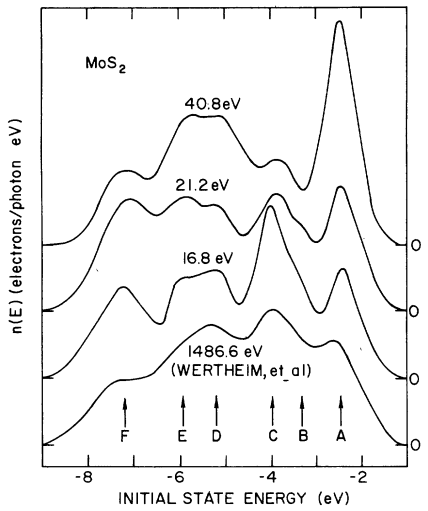

FIG. 5. EDC's from Fig. 4 with the scattering background subtracted are compared here with the XPS data of Wertheim *et al.*

Wertheim *et al.*[35] Although the subtracted background was only estimated (by extrapolating an exponential tail under the valence-band distribution), it was found that any reasonable estimate yielded the same results to within the uncertainties stated above.

Six peaks (labeled A–F) are visible in the four curves at energies of −2.5, −3.3, −3.8, −5.2, −5.9, and −7.2 eV. (The resolution of the Hewlett-Packard 5950A spectrometer used for the XPS work[35] is probably responsible for the observed "smearing" of peaks D and E in the 1486.6-eV curve. The absence of shoulder B in the 40.8- and 1486.6-eV spectra is probably due to the reduced resolution and greater noise in these spectra.)

The peak positions are the same (within experimental uncertainty) at all photon energies; however, the relative peak heights are strongly dependent on photon energy. Since final-state density effects may be small for the energies of these EDC's, the peak-height modulation is most likely caused by changes in optical-transition probabilities with changes in photon energy.

Using our notation from Fig. 1, peak A corresponds to the completely filled V_1 band, and the lower peaks correspond to the bonding valence band V_2. One of the striking features of the UPS spectrum is that the relative height of peak A (at −2.5 eV) increases markedly as the photon energy is increased from 16.8 to 40.8 eV. This type of behavior is usually associated with localized states or states with large d admixture[36] and is, therefore, consistent with a "nonbonding" d-derived uppermost filled band (V_1), as proposed in the WY model[1] (Fig. 1) and most other theoretical calculations.[3-8,10,14-16] (The d-like nature of the valence-band maximum is confirmed by electron-paramagnetic-resonance measurements by Title and Shafer.[37]) At 1486.6 eV, peak A is relatively lower again. This could be caused either by atmospheric contamination from the sample being cleaved in air (see the Appendix of this paper), or by the photoionization cross section for $4d$ electrons undergoing a so-called "Cooper minimum" due to the orthogonality of the initial- and final-state wave functions.

Because the density of states near the valence-band maximum (VBM) is very small, it is difficult to precisely locate the VBM relative to E_F. Our best estimate would place the VBM 0.9 ± 0.2 eV below E_F. Using 30 times magnification and the derivative technique described above, a very small emission signal is detected up to about 0.7 eV below E_F. Although this small signal is probably caused by analyzer resolution, it constrains the VBM to be *at least* 0.7 eV below E_F. This would be consistent with the optical measurements of Huisman *et al.*[4] which indicated a 1.35-eV band gap, rather than with the 0.27-eV band gap originally proposed by Wilson and Yoffe.[1]

Another point of controversy has been whether the nonbonding d band (V_1) overlaps the lower-bonding valence band (V_2). Wilson and Yoffe[1] originally suggested that a gap of about 1.0 eV existed between valence bands V_1 and V_2. The Mattheiss calculations also show a V_1-V_2 gap of approximately 1 eV, but he points out that this gap may be an artifact of the calculation.[14,15] No such gap is apparent in our data even when we account for the analyzer resolution. In fact, taking account of the 0.3-eV (FWHM) resolution and assuming symmetric structure for peaks A, B, and C, our data indicate that V_1 (peak A) and V_2 (peaks B–F) overlap each other by at least 0.3 eV. Such an overlap has been calculated by Kasowski[16] and by Wood and Pendry.[10]

Several other groups have published UPS data on MoS_2 at 21.2 and 40.8 eV. Williams and Shepherd[13] have published EDC's taken with several resonance lines. Williams *et al.*[12] have published EDC's from MoS_2 at 21.2 eV as a function of the angle θ between the photoemitted electrons and the c axis of the crystal. In this pioneering experiment Williams *et al.*[12] observed peaks at about the same energies reported here, except that the relative peak heights were a strong function of θ. A weighted average of their EDC's corresponds roughly to our 21.2-eV EDC shown in Fig. 5. Unfortunately, Williams *et al.*[12] give no information on the angle φ of the crystal about an axis normal to its surface, making it difficult to interpret the EDC's. Just below the Fermi level Williams *et al.*[12] further observe a weak shoulder which they identify as the nonbonding

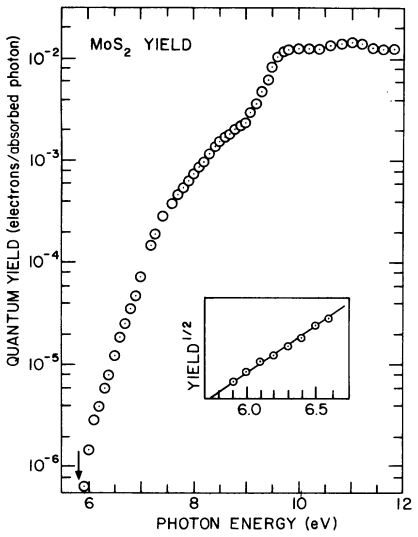

FIG. 6. Absolute photoyield of MoS_2. The inset shows the extrapolation of (yield)$^{1/2}$ to the photothreshold at 5.75 eV.

d band (V_1); but because our data show no emission within 0.7 eV of E_F, even with 30 times magnification and use of derivative techniques, we conclude that this shoulder must be caused by impurities or some other spurious effect. Our conclusion is further supported by our low-energy EDC's and our yield data presented below.

For photon energies below 11.8 eV, the photoyield of MoS_2 was measured as described above in Sec. II. Special care was taken to use filters on the monochromator to avoid any contribution to the photoyield from second-order or scattered light. Figure 6 shows the yield of MoS_2 corrected for reflectivity as measured by Liang[38] to give the number of electrons photoemitted per photon *absorbed*. All of the EDC's taken with $h\nu < 11.8$ eV have been normalized to the absolute quantum yield presented in Fig. 6. The insert shows a plot of the square root of the yield versus photon energy. This plot clearly extrapolates to a photothreshold $W = 5.75 \pm 0.1$ eV. The most unusual feature of the MoS_2 yield curve is the leveling off just below 9 eV followed by a sharp rise, which corresponds to the onset of transitions from the bonding band (V_2) to above the vacuum level (E_V). This onset of transitions is clearly visible in Figs. 7 and 8 as the peak labeled C.

If the analyzer work function Φ_A is known, the sample work function Φ can be obtained from the EDC by the relationship $\Phi = \Phi_A + V_{R_0}$, where V_{R_0} is the analyzer retarding voltage corresponding to the EDC threshold. Using the EDC from an evaporated Cu shutter on the analyzer, $\Phi_A = 4.65 \pm 0.1$ eV. From the MoS_2 EDC's we find $V_{R_0} = 0.25 \pm 0.1$ eV,

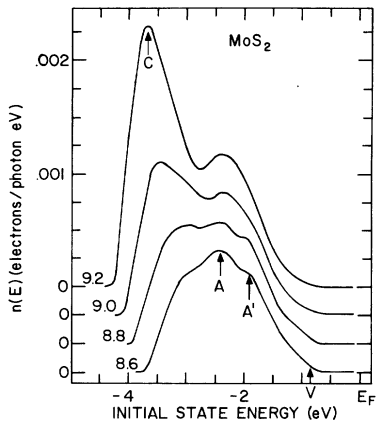

FIG. 7. EDC's showing photoemission from near the top of the MoS_2 valence band. No emission is observed above -0.7 eV, and the upper valence band (peak A) is found to overlap the lower valence band (peak C).

and thus $\Phi = 4.90 \pm 0.15$ eV. Using the threshold $W = 5.75 \pm 0.1$ eV from the yield, we find the VBM is $W - \Phi$ or 0.85 ± 0.2 below E_F, in good agreement with the value 0.9 ± 0.2 eV determined above directly from the high-energy EDC's.

Williams and McEvoy (WM) have reported[11] photoyield data for clean MoS_2 which are similar to

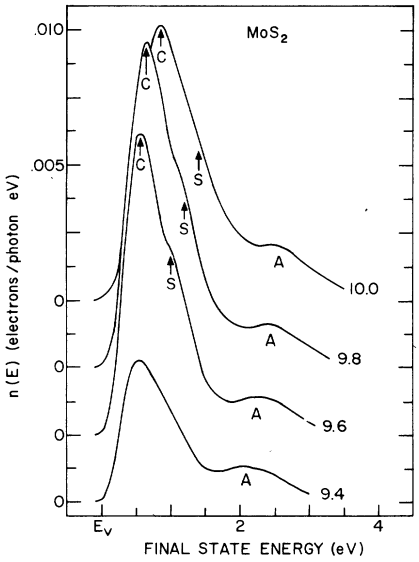

FIG. 8. EDC's showing the rapid rise of peak C for photon energies up to 9.8 eV. [Note that the vertical scales for each EDC have been offset from each other by 0.0025 electron/(photon eV). Thus, peak C at 9.8 eV has $n(E) = 0.012$ electrons/(photon eV).] The EDC's are plotted as a function of the electrons' final-state energy above the vacuum level (E_v). In this type plot, a structure such as A or S, which moves directly with photon energy, corresponds to a constant initial-state energy.

ours for photon energies above 7 eV. Below 7 eV, however, WM observe a much higher yield which persists to a threshold of 4.55 eV, about 1.2 eV below what we observe. By comparing our EDC's in Figs. 7 and 8 with EDC's reported by WM, we find that they observe the vacuum level 0.5 eV lower than we do when referenced to corresponding sharp structures or E_F in the respective EDC's. This could easily be caused by slightly different surface conditions and does not change any conclusions about the electronic structure. The remaining 0.7-eV discrepancy is in the energy of the VBM relative to E_F (or relative to lower-lying sharp structure). Since the energy of the VBM below E_F sets the lower limit on the size of the forbidden gap, we took special care to verify our data near the photothreshold. Small effects had to be considered here because the level of yield in the disputed region was very small—more than three orders of magnitude below the yield a few eV above threshold. We used unusually pure crystals[34] and found it imperative to use filters to eliminate scattered and second-order light from the monochromator. The removal of the filters gave the apparent effect of lower threshold. We suggest that this effect or sample impurities might have been responsible for the low threshold observed by WM.[11]

Figure 7 shows peak A from band V_1 to be 2.5 eV below E_F with a weak shoulder A' on the high-energy side of A (at −2.0 eV). As with the high-energy EDC's, the "tailing" of the valence band makes it difficult to determine the VBM very precisely; however, the curves in Fig. 7 still show the VBM at least 0.7 eV below E_F, and they are consistent with the more precise determination of −0.85 eV from the yield data. Even with the higher resolution obtained at these energies, there still appears to be a few tenths eV overlap of band V_1 (peak A) with the top of the lower bonding band V_2 (peak C).

From the shape of peak A, we have good evidence that the valence-band maximum occurs at Γ in the Brillouin zone rather than near a zone edge. For a simple band, Fig. 9(a) shows the density of states $n(E)$ expected when the VBM is at Γ; and Fig. 9(b) shows the case when the VBM is near the zone edge. The similarity of the observed shape of peak A to that of $n(E)$ in Fig. 9(a) strongly suggests that in MoS_2 the VBM is at Γ, as calculated by Kasowski[16] and Mattheiss[14,15] [Fig. 9(c)], rather than near a zone edge as deduced by some others.[1,6-8] Over a limited energy range, the shape of peak A could be influenced by matrix-element or final DOS effects, but the observation of the same characteristic shape for all $h\nu$ supports the assertion that the shape arises from $n(E)$ and, hence, that the

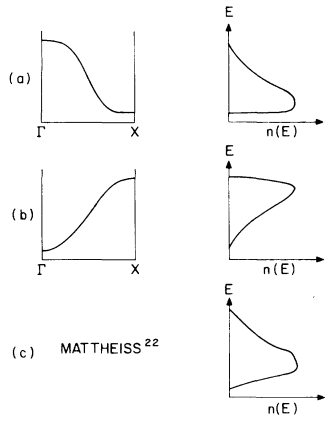

FIG. 9. Density of states $n(E)$ expected (a) for the case of VBM at Γ and (b) for VBM near a zone edge. (c) Shows $n(E)$ calculated by Mattheiss.

VBM is at Γ.

Figure 8 shows a rapid rise in the height of peak C near the photothreshold until it reaches a maximum for a photon energy of 9.8 eV. In this figure the EDC's are plotted as a function of the electrons' final-state energy above the vacuum level (E_V) so that an EDC structure such as A or S which moves directly with photon energy corresponds to structure in the initial density of states. If peak C were due to a high initial density of states it would also move directly with photon energy in this plot. Below 9.8 eV, however, peak C appears stationary because it is partially hidden below the vacuum level and only the leading edge is visible. Above 9.8 eV the top of peak C is exposed and observed to move with photon energy indicating a constant initial-state origin over the photon energy range 9.8–10.0 eV. The fivefold increase in the height of peak C between 9.2 and 9.8 eV is not unusual for peaks near threshold; however, peak C decreases almost as rapidly as the peak starts to move above the threshold (Fig. 10). This striking rise and decay of a peak in a photon energy range of about 1 eV is a strong indication that the peak corresponds to a direct interband transition.[33] Figure 10 also shows that, as the photon energy is increased further, lower-lying structures are exposed at the same initial-state energies where structures were observed in the resonance lamp curves above (Fig. 5).

The data from all of the MoS_2 EDC's are conveniently summarized in the "structure plot" shown in Fig. 11, where the initial-state energy of each piece of structure has been plotted as a function of photon energy. (The high-energy end of the horizontal scale has been compressed to make the figure more compact.) Different symbols are used on the plot to roughly indicate the relative peak

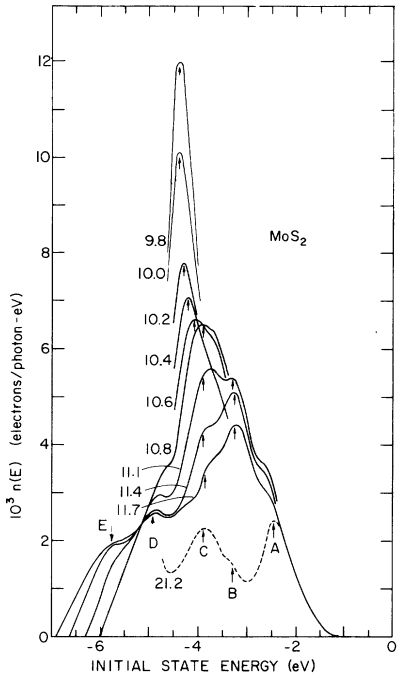

FIG. 10. EDC's for photon energy 9.8–11.7 eV plotted vs initial-state energy with all curves having the same zero for $n(E)$. Because these EDC's overlap, only the important portions of some curves are shown.

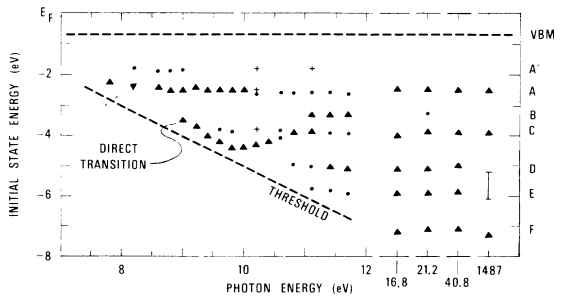

FIG. 11. MoS_2 structure plot showing EDC peak positions as a function of photon energy. This high-energy end of the horizontal scale has been compressed to make the figure more compact. Triangles are used to indicate peaks, dots indicate shoulders, and crosses indicate structure on derivative curves. With the exception of peak C, the structures are all clustered about lines of constant initial-state energy.

heights.

With the exception of peak C, the peaks are closely clustered about lines of constant initial-state energy over a wide range of $h\nu$, where the final density of states (DOS) and optical-transition probabilities are expected to vary drastically. This indicates that peaks *other than C* correspond to structure (probably peaks) in the valence-band density of states[33] of MoS_2 at −1.9, −2.5, −3.3, −5.2, −5.9, and −7.2 eV.

The behavior of peak C requires more careful attention. Above $h\nu = 11$ eV, peak C is observed at a constant initial-state energy. This persistent appearance of structure at −3.9 eV is good evidence that a peak in the valence-band DOS exists at 3.9 eV below E_F. Below $h\nu = 11$ eV, the high initial-state density (HISD) at - 3.9 eV gives rise to the weak shoulder S (indicated by dots and crosses in Fig. 11) and the large peak C is observed at an apparent initial-state energy as low as −4.4 (when $h\nu = 9.8$ eV). Since no structure is observed at −4.4 eV with other photon energies it is unlikely that a HISD exists there. It is equally unlikely that a high final-state density 1 eV above threshold is completely responsible for the behavior of peak C; because, if that were the case, other peaks would experience enhancement at the same final-state energy. Instead, such an energy shift and dramatic height modulation over a small photon energy range is usually associated with a direct interband transition.[33] For this direct transition case the sharp increase in peak height can occur when the valence and conduction band are nearly parallel and a narrow range of photon energies can excite electrons over a large volume of the Brillouin zone.

Although we have interpreted the EDC peak positions with a density-of-states model and found the increasing height of peak A with photon energy consistent with a mainly d-like upper valence band, a more detailed interpretation of the peak-height modulation and the direct-transition peak will require an accurate calculation of MoS_2 band structure and transition probabilities.

It has been suggested by Yoffe[2] that UPS data may give ambiguous results since the electron-energy levels near the surface can be different from the bulk.[10,39] From our photoyield data and optical-absorption results, we can roughly estimate an "escape depth" (equivalent to sampling depth) of only a few angstroms—about one sandwich layer—at $h\nu \sim 11$ eV. This estimate is supported by angular UPS measurements on $TaSe_2$ by Smith and Traum[22] who attribute the residual threefold symmetry to an escape depth less than two sandwich thicknesses. This surface selectivity of our UPS data would be of concern except for the fact that our data are in excellent agreement with the XPS data at 1486.6 eV,[35] where the "escape depth" is expected to be much longer,[40] thereby sampling the electronic structure of at least several complete layers. If our estimate of the UPS escape length is correct, this would imply that the electronic DOS structure of the first layer is not too different from the bulk structure. Williams and McEvoy[11] have reached the same conclusion after noting the similarity of electron energy-loss spectra at 100 eV

and 80 keV. This possibility is not too surprising in MoS_2 because of the relatively weak interlayer interaction. Thus, our UPS location of peaks in the valence-band density of states ought to be indicative of the *bulk* DOS in $2H$-MoS_2.

IV. COMPARISON OF MoS_2 PHOTOEMISSION DATA WITH OTHER EXPERIMENTAL RESULTS

Although photoemission (UPS) is one of the most useful techniques for the study of filled electronic states, it has not been possible (in the case of MoS_2) to extract much information on the nature of the unfilled conduction-band states from the UPS data alone; but, by combining the UPS data with data from other optical methods, considerable information on these conduction-band states can be obtained.

Soft-x-ray absorption spectroscopy (XAS), which yields conduction-band information directly, has been applied to MoS_2 by Sonntag and Brown[41] and by Barinskii and Vainshtein.[42] Since the initial states of XAS transitions are core levels of well-defined atomic character, electric-dipole selection rules can be used to *estimate* the relative atomic character in final conduction-band states. One must be cautious, however, since strong hybridization effects which have been calculated[14,15] for MoS_2 would make the symmetry of the final-state wave functions more dependent on band-structure effects than pure atomic characters. A further caution in correlating XAS features and conduction-band structure is that considerable energy shift or distortion of the edge could be caused by excitonic effects.[43,44] Although we will not consider these effects here, we point out that they may invalidate conclusions which require exact correspondence of the energies of structures in XAS spectra with the conduction bands.

The sulfur L_{II}, L_{III} XAS data of Sonntag and Brown[41] (SB) in Fig. 12(a) show a two-peaked structure (C_{1A} and C_{1B}) about 4 eV wide at the absorption edge for transitions from the sulfur $2p$ core levels. (The spin-orbit splitting of the core level has been deconvolved from this spectrum.) The two-peak structure is followed by a sharp rise in absorption for higher photon energies. SB suggest that the double-peaked structure which they observe corresponds to transitions into the lower conduction band C_1 (see Fig. 1). This band is predicted to be "Mo d-like" in most MoS_2 band models and calculations[1,3-8,10,14-16]; but this band has some sulfur s or Mo p character for the structure to appear in the sulfur $L_{II,III}$ edge. The sharp rise in absorption which SB observe about 5 eV above the edge corresponds to transitions into the upper conduction-band states C_2. The transition energy locates the bottom of the C_2 band near the vacuum level reported in this work. The strength of the transitions into C_2 is consistent with a predominant sulfur s character in C_2, as predicted by most models.[1,3-8,10,14-16]

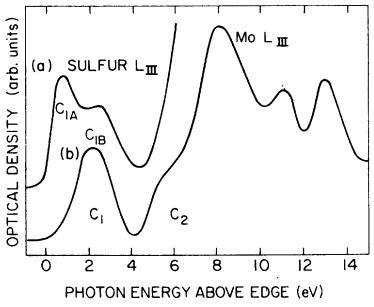

FIG. 12. Comparison of x-ray absorption edges in MoS_2. (a) Sulfur L_{III}-edge data of Sonntag and Brown. (b) Molybdenum L_{III} edge of Barinskii and Vainshtein.

Barinskii and Vainshtein[42] have reported a somewhat similar absorption-edge structure (although they observed a narrower unresolved peak corresponding to C_1) even though they were looking at transitions from p states on the Mo atoms [Fig. 12(b)]. One would expect transitions from the Mo p states to the "d-like conduction bands" (C_1), but the relatively strong transitions to C_2 indicate that the conduction-band states in C_2 must include considerable admixture of Mo 5s or 4d character in addition to the predominant sulfur s character suggested by the data of SB.[41] The mainly sulfur s character of C_2 would also be consistent with the strong "direct-transition" peak we observed in our UPS data from mainly sulfur p-like V_2 to C_2. One important conclusion from the XAS data must be that the conduction bands (and therefore, probably, the valence bands) are strongly hybridized, making it difficult to assign optical transitions using simple atomic-orbital models and atomic selection rules.

Since MoS_2 is a semiconductor, the filled states (observed by photoemission) and the empty states (observed by XAS) are separated by a large band gap rather than being continuous across the Fermi level (E_F) as in a metal. Therefore, it is important to have optical-absorption data $\alpha(h\nu)$ in the 1–12-eV range to find the energy separation of the experimentally observed filled and unfilled states so that a complete electronic-structure model can be formulated. As indicated above, one must be cautious when using the optical-absorption data to connect the UPS and XAS data since exciton effects in the XAS can shift the apparent absorption edge by as much as 1 eV. Thus, correspondence of structures well above the absorption edge is more meaningful than at the edge itself. Since no optical-ab-

sorption data on MoS_2 have been published for photon energies above 4 eV, reflectivity measurements must be used to calculate $\alpha(h\nu)$ from the Kramers-Kronig (KK) relations.[44] Fortunately, various measurements of the near-normal-incidence optical reflectivity $R(h\nu)$ for MoS_2 have been published,[38,46,47] one for photon energies up to ~70 eV.[46] The KK calculation was performed using a computer program which has been described by Bauer.[48] We chose what appeared to be the most reliable data in each range of photon energy and combined them into a composite $R(h\nu)$ curve from 0 to 70 eV. The synchrotron-radiation data of Leveque *et al.*[46] were chosen for the 15–70-eV range, and the data of Liang[38] were chosen for the 4–12-eV range. The data of Liang[38] and the data of Leveque *et al.*[46] agreed almost exactly when each was smoothly extrapolated into the 12–15-eV region. In the range 1.5–4 eV, the room-temperature data of Sobolev[47] were used, but they were scaled up by a factor of 1.8 so that they would match Liang's data in the 4.0 ±0.3-eV overlap region. Below 1.5 eV the reflectivity was extrapolated smoothly to 32% at $h\nu = 0$ as estimated from the dielectric constant. [A plot of the composite $R(h\nu)$ used for our KK calculation is shown in Fig. 13.] Since it was found that the results of the KK calculation above 4 eV were changed only slightly (changes in α of ~2%) for any reasonable fitting of the data below 3 eV, our calculated values for α above 4 eV are probably accurate to a few percent (assuming, of course, that the data of Liang, and Leveque *et al.* are exact). Below 4 eV, however, our calculated α is uncertain to ~±50%, and it agrees only qualitatively with direct measurements of α in the range ~2–4 eV.[1,49]

Figure 14 shows the optical absorption $\alpha(h\nu)$ between 0 and 12 eV as calculated by the Kramers-Kronig program.[48] The most noticeable feature of the absorption is the sharp dip in α at 9 eV followed by a sharp rise to 10 eV. This sharp rise (labeled 5 in Fig. 14) occurs at the same photon energy as the sharp rise in the yield reported above in Sec. III, where we have argued that this is the

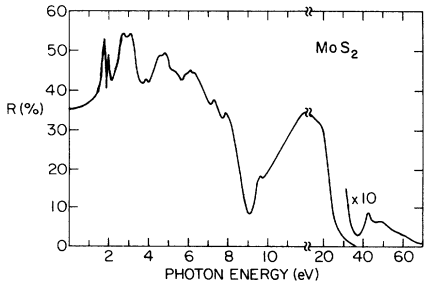

FIG. 13. Composite reflectivity for MoS_2 used in Kramers-Kronig analysis. The various data sources are given in the text.

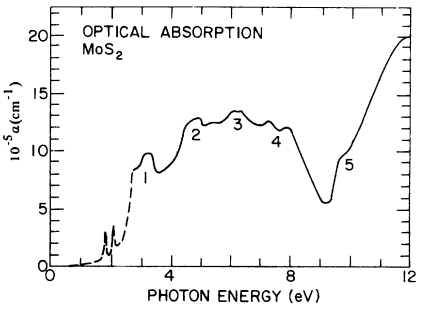

FIG. 14. Optical absorption $\alpha(h\nu)$ of MoS_2 calculated from reflectivity (Fig. 13) using Kramers-Kronig relations.

onset of transitions from the lower valence band (V_2 in Fig. 1, peak C in the EDC's) to states C_2 near the vacuum level about 5 or 6 eV above E_F. Peak 1 between 2.5 and 3.5 eV is assigned to transitions from the upper filled band V_1 (peak A in the EDC's) to the bottom of the conduction band C_{1A} (Fig. 12). Peak 2 has contributions from both VB peak A to C_{1B} and VB peak C to C_{1A}. Peak 3 then corresponds to transitions from peak C to C_{1B} and peaks D and E to C_{1A}. And, finally, peak 4 results from transitions from D and E to C_{1B} and F to C_{1A}. These assignments are different from those suggested by some other groups.[1,49]

The dip in α at about 9 eV has been previously assigned to a plasmon.[38] Indeed, the energy loss function $-\mathrm{Im}(\epsilon^{-1})$ computed from the KK relations, shows a plasmon-loss peak at 8.7 eV, in good agreement with the loss function determined by electron-energy-loss spectroscopy (ELS) measurements taken with the transferred wave vector q perpendicular to the c axis.[50]

We have used the KK program to compute ϵ_2, the imaginary part of the dielectric constant of MoS_2. Figure 15 shows ϵ_2 (solid line) computed by our KK

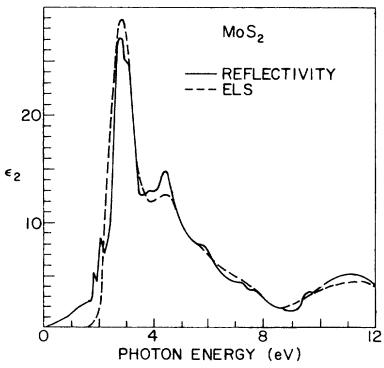

FIG. 15. Comparison of ϵ_2 computed from R (solid line) with ϵ_2 computed from ELS (dashed line). Although the ELS shows less resolution, the overall features are in remarkable agreement.

program to be in remarkable agreement with ϵ_2 computed from ELS data (dashed)[50] with $\vec{q} \perp \vec{c}$ (except that the ELS data are not as high resolution as the optical data). Since ELS data and the optical data agree so well for the case of light polarized perpendicular to the c axis, it reassures the use of ELS data with $\vec{q}$ parallel to $\vec{c}$ (Ref. 50) to obtain the optical constants over a wide range for the case of light polarized *parallel* to the c axis, which has been unobtainable in any energy range because of the thinness of available MoS_2 crystals. High-resolution ELS data can lead to the availability of optical constants for both polarizations, which will, in the future, greatly aid the interpretation of optical-absorption data in terms of detailed band structure.

Having presented our UPS data and expanded on the published optical data, we are in a position to use these data to construct an experimental electronic structure model for $2H$-MoS_2. This model will be discussed in Sec. V.

V. MoS_2 CONCLUSIONS

Figure 16 shows our band model (labeled MS) for MoS_2. We have taken the zero of the energy scale to be at our best estimate of the valence-band maximum. Although the valence-band density of states plot in the figure is only schematic, the peaks in the plot probably correspond to peaks in the DOS.

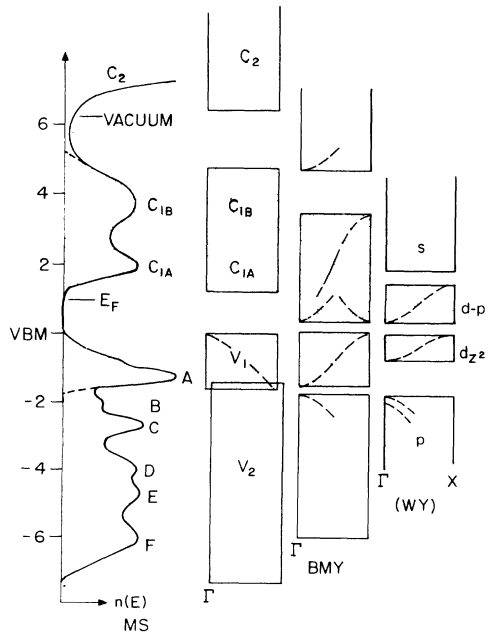

FIG. 16. Experimental band model derived from the present work (MS) compared with the Wilson-Yoffe model and a semiempirical calculation based on WY by Bromley, Murray, and Yoffe (BMY).

The peak heights are not to scale and are only estimates based on the average relative EDC peak heights over the range of photon energies studied. More accurate determination of valence-band DOS peak heights cannot be made without knowledge of transition-matrix elements from a detailed electronic-structure calculation.

The conduction-band structure is even more uncertain in both relative peak heights and absolute energy position. The model for the conduction-band DOS relies heavily on the XAS data.[41] Our photoemission data support the existence of a high density of conduction-band states just above the vacuum level, but no other conduction-band features could be established from trends in EDC peak heights as a function of final-state energy. The absolute energy of the conduction-band minimum is determined by correlating valence- and conduction-band DOS peaks (from photoemission and XAS, respectively,) with peaks in the optical-absorption data. The resultant band gap is close to the 1.35-eV gap reported by Huisman *et al.*[4]

Unfortunately, no complete DOS calculations are available in the literature for comparison with our experimental DOS. We will, however, compare our band model with the Wilson-Yoffe[1] model and models adapted from some of the more recent band calculations. Since none of the calculations is in good agreement with all aspects of our experimental model, we cannot single out a "correct" calculation. Instead, we will discuss similarities of each calculation with an eye toward understanding how differences arise between the calculations and experiment. Since all the models fit the similar arrangement of a two-part valence band and a two-part conduction band, we shall use the labeling scheme of Fig. 1 when discussing the models.

The original Wilson-Yoffe model[1] (WY) and the semiempirical calculation of Bromley, Murray, and Yoffe[7] (BMY) are included in Fig. 16 for comparison with our experimental model. The BMY calculation fits a tight-binding approximation to the semiconducting gap energy and the V_2 to C_{1A} transition energy of the WY model by adjusting the tight-binding matrix elements with a set of reduction parameters. This accounts for the exact agreement of these energies in the two models. Before the availability of MoS_2 photoemission data it was reasonable to fit a calculation to the WY model since that model could explain many of the trends in TX_2 optical data. However, the unusually large reduction factor corrections required to effect the fit should have been a clue that the WY model might not be correct. We note, however, that the V_1 and C_1 bandwidths of the BMY "calculation" are close to the experimental observations. Another semiempirical calculation by Edmondson[8] is

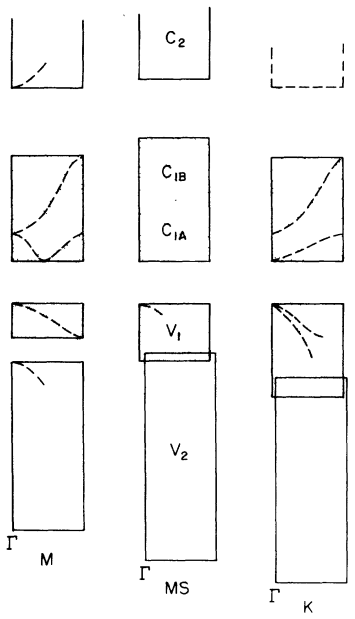

FIG. 17. Comparison of MS model with "first-principles" calculations by Mattheiss (M) and Kasowski (K).

similar in method and results to that of BMY.[7]

In Fig. 17 our model (MS) is compared to the "first-principles" calculations of Mattheiss[14,15] and Kasowski.[16] Both of these calculations use the same atomic potentials, however, Kasowski's linear-combination-of-muffin-tin-orbitals method can include much more of the nonspherical part of the potential than Mattheiss's augmented-plane-wave (APW) calculations. It is encouraging that the essential features of these *a priori* calculations are in agreement with our experimental model. The differences are apparently due to peculiarities of the two calculations.

Kasowski's calculation agrees well with our photoemission data near the band gap (i.e., the *d*-band manifold); however, his V_2 valence band extends to lower energy than in the photoemission. This low-energy part of V_2 is in the M to L region of the Brillouin zone, where the V_1 band also extends to much lower energy than photoemission suggests. These effects may be due to a systematic feature of Kascowski's calculation.[16] Although Mattheiss calculates too narrow a V_1 band, which does not overlap the V_2 band, he attributes this to the fact that the APW method is less reliable in predicting relative energies of d and s-p bands.[15]

Perhaps the most valuable contribution of Mattheiss's papers[14,15] was his linear-combination-of-atomic-orbitals investigation of the *d*-band manifold. His calculations showed for the first time that the large band gap was primarily due to a strong hybridization of the Mo *d* bands and not the ligand-field splitting. A more thorough comparison of these calculations with experiment is almost impossible without detailed computation of the density of states and matrix elements.

Another approach toward an understanding of MoS_2 energy levels might be a molecular-orbital calculation of the type successfully applied to analysis of TiS_2 by Fischer.[51] Although molecular-orbital calculations may have trouble reproducing features such as the hybridization gap, they may be useful in determining the origin of DOS peaks in angle-integrated photoemission data and XAS data.

Our experimental band model has been shown to be representative of the bulk electronic structure of $2H$-MoS_2 within the limitations discussed above. Two controversial aspects of MoS_2 have been unambiguously determined; namely, the large (> 1-eV) band gap and the overlap of the V_1 and V_2 bands. Our location of peaks in the valence-band density of states, the dependence of peak heights on photon energy, and the behavior of peak C ought to provide a sensitive test for a detailed calculation of bulk DOS and optical-transition probabilities for $2H$-MoS_2.

APPENDIX: EFFECTS OF SURFACE CLEANLINESS ON PHOTOEMISSION RESULTS FROM MoS_2

Since the cleaved MoS_2 surface is extremely inert, it has often been assumed that no special precautions need to be taken when preparing an MoS_2 sample for photoemission experiments. In this appendix we present photoemission data at 21.2 and 40.8 eV taken on MoS_2 samples with surfaces prepared in various ways. Our results will be compared with other data on MoS_2 surface contamination reported in the literature.

For an investigation of the adsorption of gases on an MoS_2 substrate[52,53] it was desired to have a simple method of repeatedly preparing a fresh atomically clean MoS_2 surface without the necessity of breaking vacuum, as was required with the cleaving method. Since heating in ultrahigh vacuum has been used successfully in many other cases to prepare atomically clean surfaces, this method was tried first.

The large MoS_2 natural single crystals were first ultrasonically degreased in successive baths of trichloroethylene, acetone, and methanol. After removing them from the methanol, they were blown dry with dry nitrogen and kept for several days in a dry nitrogen atmosphere at 100 °C. Immediately prior to pumping down the vacuum, the samples were cut with a sharp razor blade to fit the sample holder and then cleaved with a piece of cellophane tape to expose a fresh surface. Within five minutes of cleaving, the pressure in the chamber was re-

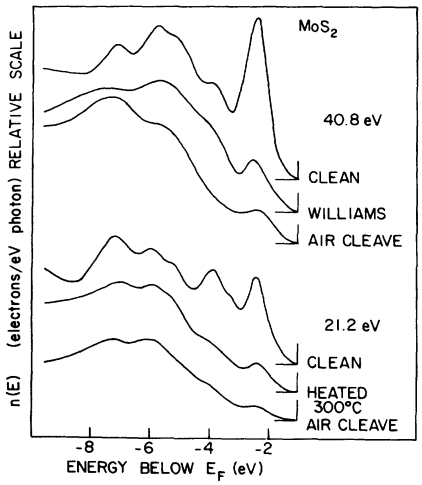

FIG. 18. Comparison of EDC's at 21.2 and 40.8 eV on samples of MoS_2 in various stages of cleanliness.

duced to approximately 10^{-5} Torr. In approximately 2 h the pressure was reduced to 10^{-7} Torr, and photoelectron energy-distribution curves could be measured. The EDC's at 10^{-7} Torr were almost completely smeared out from those observed on samples cleaved in UHV. Furthermore, the number of secondary photoelectrons emitted was about three lines larger than in the cleaved samples. Surprisingly, as the chamber was pumped to lower pressures, the EDC's sharpened significantly, and the number of secondary electrons was reduced. Obviously, some of the surface contaminants are so weakly bound that they desorb in vacuum even at room temperatures. Typically, the small photoemission chamber was pumped to about 5×10^{-10} Torr in 5–6 h, at which time the general peaks in the EDC's could be discerned. Figure 18 shows such EDC's (labeled AIR CLEAVE) taken with photon energies of 21.2 and 40.8 eV.

As the samples were heated to increasingly higher temperatures (and cooled to room temperature before measurements), the EDC's were observed to sharpen. In Fig. 18 the 21.2-eV EDC from a sample heat-cleaned for a few minutes at 300°C is clearly sharper than the air-cleaved sample at the same photon energy. After many trials, it was found that heat-cleaning at 400 to 450°C for a period of 6 h yielded EDC's essentially identical to EDC's from samples cleaved in UHV. Fig. 18 clearly shows the sharper, more detailed structure indicative of an atomically clean surface.

We should point out that cleaving in vacuum is not a foolproof technique. Figure 18 includes a 40.8-eV EDC taken by Williams and Shepherd[13] on a sample which they cleaved in UHV. By comparison with the other curves in Fig. 18, it appears that their sample was not completely clean. This could easily occur from only part of the illuminated area of the sample being peeled away during the cleaving process; or the sample may have cleaved along a region where impurities were included between the MoS_2 layers.

Wertheim *et al.*[35] have observed sharp EDC's from air-cleaved MoS_2 samples at 1486.6 eV. This is possible because of the much greater escape depth for electrons with ~1400-eV kinetic energy. At 21.2 and 40.8 eV the primary photoelectrons have escape depths on the order of one sandwich thickness, so even a small amount of surface contamination results in a large percentage effect on the EDC's. With ~1400-eV kinetic energy, electrons are expected to have much greater escape lengths—perhaps as much as 50-100Å.[40] In that case even a full monolayer of contamination contributes only a small percentage of the total photoemission, and so it has little effect on the observed EDC.

Attempts to observe surface contamination on MoS_2 using Auger-electron spectroscopy (AES) usually indicate no N_2, O_2, or C even on air-cleaved samples.[54,55] The most likely reason for this is that the incident electron beam necessary to excite the Auger transitions also desorbs most of the contaminants before a spectrum can be taken. Perhaps the most promising method for studying MoS_2 surface contamination is to use synchrotron radiation to excite core electrons from contaminants. By proper choice of photon energy, this technique can be highly surface sensitive (escape depth ~1 sandwich thickness), while at the same time causing far less desorption of contaminants than an electron-beam probe.

†Work supported by the U.S. AFOSR and by the U. S. Army Research Office under Grant No. DAHC04-74-6 0215.

*Present address: Xerox Palo Alto Research Center, Palo Alto, Calif. 94304.

[1]J. A. Wilson and A. D. Yoffe, Adv. Phys. 18, 193 (1969).

[2]A. D. Yoffe, Festkoerperprobleme 13, 1 (1973); Ann. Rev. Mater. Sci. 3, 147 (1973).

[3]J. B. Goodenough, Phys. Rev. 171, 466 (1968); Mater. Res. Bull. 3, 409 (1968).

[4]R. Huisman, R. deJonge, C. Haas, and F. Jellinek, J. Solid State Chem. 3, 56 (1971).

[5]G. A. N. Connell, J. A. Wilson, and A. D. Yoffe, J. Phys. Chem. Solids 30, 287 (1969).

[6]R. A. Bromley, Phys. Lett. A 33, 242 (1970).

[7]R. A. Bromley and R. B. Murray, J. Phys. C 5, 739 (1972); R. A. Bromley, R. B Murray, and A. D.

Yoffe, *ibid.* 5, 759 (1972).
[8]D. R. Edmonson, Solid State Commun. 10, 1085 (1972).
[9]J. C. McMenamin and W. E. Spicer, Phys. Rev. Lett. 29, 1501 (1972).
[10]K. Wood and J. B. Pendry, Phys. Rev. Lett. 31, 1400 (1973).
[11]R. H. Williams and A. J. McEvoy, Phys. Status Solidi B 47, 217 (1971); J. Phys. E 4, 446 (1971).
[12]R. H. Williams, J. M. Thomas, M. Barber, and N. Alford, Chem. Phys. Lett. 17, 142 (1972).
[13]P. M. Williams and F. R. Shepherd, J. Phys. C 6, L36 (1973); F. R. Shepherd and P. M. Williams, *ibid.* 7, 4427 (1974).
[14]L. F. Mattheiss, Phys. Rev. Lett. 30, 784 (1973).
[15]L. F. Mattheiss, Phys. Rev. B 8, 3719 (1973).
[16]R. V. Kasowski, Phys. Rev. Lett. 30, 1175 (1973); and private communication.
[17]R. J. Powell, Ph.D. thesis (Stanford University, 1976) (unpublished), Xerox Univ. Microfilms No. 67-17484.
[18]G. F. Derbenwick, Ph.D. thesis (Stanford University, 1970) (unpublished), Xerox Univ. Microfilms No. 72-12882.
[19]R. C. Eden, Rev. Sci. Instrum. 41, 252 (1970).
[20]A. Liebsch, Phys. Rev. Lett. 32, 1203 (1974); Phys. Rev. B 13, 544 (1976); J. W. Gadzuk, *ibid.* 10, 5030 (1974); Solid State Commun. 15, 1011 (1974).
[21]H. P. Hughes and W. Y. Liang, J. Phys. C 6, 1684 (1973).
[22]N. V. Smith and M. M. Traum, Phys. Rev. B 11, 2087 (1974).
[23]M. M. Traum, N. V. Smith, and F. J. DiSalvo, Phys. Rev. Lett. 32, 1241 (1974).
[24]A. L. Sommer and W. E. Spicer, in *Methods of Experimental Physics*, edited by L. Marton (Academic, New York, 1959), Vol. 6B.
[25]Indium alloy solders were obtained in a Research Solder Kit from Indium Corp. of America, P. O. Box 269, Utica, N.Y. 13403.
[26]This technique was suggested by R. E. Howard, Stanford University (private communication).
[27]K. Y. Yu, Ph.D. thesis (Stanford University, 1976) (unpublished), Xerox Univ. Microfilms No. 76-26097.
[28]D. Collins (private communication).
[29]D. E. Eastman and J. J. Donelon, Rev. Sci. Instrum. 41, 1648 (1970).
[30]The 2-mm thick cleaved LiF plate was cemented into a silver ring with "Vac-Seal" epoxy and mounted on a Varian vacuum flange.
[31]G. B. Fisher, W. E. Spicer, P. C. McKernan, V. F. Pereskok, S. J. Wanner, Appl. Opt. 12, 799 (1973).
[32]A. D. Baer, Ph.D. thesis (Stanford University, 1971) (unpublished) Xerox Univ. Microfilms No. 72-05883.
[33]C. N. Berglund and W. E. Spicer, Phys. Rev. 136, A1030 (1964); W. E. Spicer, J. Res. Nat. Bur. Standards A 74, 397 (1970).
[34]J. V. Acrivos (private communication).
[35]G. K. Wertheim, F. J. DiSalvo, and D. N. E. Buchanan, Solid State Commun. 13, 1225 (1973).
[36]H. Ehrenreich, H. R. Philipp, and B. Segall, Phys. Rev. 132, 1918 (1963); and G. K. Wertheim, L. F. Mattheiss, M. Campagna, and T. P. Pearsall, Phys. Rev. Lett. 32, 997 (1974).
[37]F. Mehran, R. S. Title and M. W. Shafer, Solid State Commun. 20, 369 (1976); and R. S. Title and M. W. Shafer, Phys. Rev. Lett. 28, 808 (1972).
[38]W. Y. Liang, J. Phys. C 4, L378 (1971); H. P. Hughes and W. Y. Liang, *ibid.* 7, 1023 (1974).
[39]D. J. Chadi and M. L. Cohen, Phys. Rev. B 11, 732 (1975).
[40]I. Lindau and W. E. Spicer, J. Electron. Spectrosc. Relat. Phenom. 3, 409 (1974).
[41]B. Sonntag and F. C. Brown, Phys. Rev. B 10, 2300 (1974).
[42]R. L. Barinskii and E. E. Vainshtein, Izk. Akad. Nauk. SSR Ser. Fiz. Mat. Nauk. 21, 1375 (1957) [Acad. Sci. USSR 21, 1375 (1957)].
[43]R. S. Bauer, R. Z. Bachrach, J. C. McMenamin, and D. E. Aspnes, Nuovo Cimento (to be published).
[44]A. B. Kunz, J. Phys. C 7, L231 (1974).
[45]M. Cardona, in *Optical Properties of Solids*, edited by S. Nudelman and S. Mitra (Plenum, New York, 1969).
[46]G. Leveque, S. Robin-Kandare, L. Martin, and F. Pradal, Phys. Status Solidi B 58, K65 (1973).
[47]V. V. Sobolev, Opt. Spectrosk. 18, 334 (1965) [Opt. Spectrosc. 18, 187 (1965)]; V. V. Sobolev, V. I. Donetskikh, A. A. Opalovskii, V. E. Fedorov, E. V. Lobkov, and A. P. Mazhara, Fiz. Tek. Pol. 5, 1025 (1971) [Sov. Phys.-Semicond. 5, 909 (1971)].
[48]R. S. Bauer, Ph.D. thesis (Stanford University, 1970) (unpublished), Xerox Univ. Microfilms No. 71-19646; (private communication); R. S. Bauer, W. E. Spicer, J. J. White, III, J. Opt. Soc. Am. 64, 830 (1974).
[49]A. R. Beal, J. C. Knights, and W. Y. Liang, J. Phys. C 5, 3540 (1972).
[50]K. Zeppenfeld, Opt. Commun. 1, 377 (1970).
[51]D. W. Fischer, Phys. Rev. B 8, 3576 (1973).
[52]K. Y. Yu, J. C. McMenamin, and W. E. Spicer, J. Vac. Sci. Technol. 12, 286 (1975).
[53]K. Y. Yu, J. C. McMenamin, and W. E. Spicer, Surf. Sci. 50, 149 (1975).
[54]R. H. Williams and A. J. McEvoy, J. Phys. D 4, 456 (1971).
[55]H. C. Feng and J. C. Chen, J. Phys. C 7, L75 (1974).